



## Rock fall Susceptibility Mapping Using Artificial Neural Network, Frequency Ratio, and Logistic Regression: A Case Study in Central Iran, Taft County

M. Mokhtari<sup>1\*</sup>, S. Abedian<sup>2</sup>, S.A. Almasi<sup>1</sup>

<sup>1</sup>Department of Civil Engineering, Faculty of Engineering, Yazd University, Yazd, Iran

<sup>2</sup>Instructor of University of Environmental Sciences, Department of Agriculture and Natural Resource, University of Payam-e-noor, Kerman branch, Iran

**ABSTRACT:** This study aims at evaluating and comparing the ability of Artificial Neural Network (ANN), Logistic Regression (LR), and Frequency Ratio (FR) methods to generate a rock fall susceptibility map for predicting the probability of rock fall occurrences in Taft County, a central region of Iran. The maps were prepared by assuming an association between rock fall susceptibility and nine factors including slope angle, slope aspect, elevation, land use, lithology, precipitation, distance from faults, distance from roads, and distance from streams. The performance of the methods was evaluated using the area under the operating characteristic curve (ROC), the precision of the predicted results (P), seed cell area index (SCAI) and statistical measures, including sensitivity, specificity, and accuracy. The area under the ROC was calculated for the frequency ratio, the artificial neural network, and logistic regression methods, and it was found to be 0.899, 0.893, and 0.883, respectively. An assessment of the parameter P also showed the high precision of all the three methods (particularly the frequency ratio method) for identifying high-susceptibility areas. It was also found that high-susceptibility classes had low SCAI values in all the methods, while low-susceptibility classes had higher SCAI values indicating acceptable performance of models. Overall, the results showed that the model developed by the FR method has better prediction accuracy than the ANN and LR methods. Decision makers can effectively use the findings of the present study to mitigate the financial and human cost resulting from the rockfalls.

### Review History:

Received: 2018-12-01

Revised: 2018-12-31

Accepted: 2019-03-12

Available Online: 2019-03-12

### Keywords:

Rock fall susceptibility map

Artificial neural network

Logistic regression

Frequency ratio

Taft County

## 1. INTRODUCTION

Rock fall is a mass movement of the rock falling from the cliff face. It can be classified as a small type of landslide limited to freely detached rocks [1]. Rock fall is a frequent phenomenon happening in mountainous regions, threatening human lives and foundations. Rock fall or rock slide may lead to large scale mass motions of rock fragments; this, in turn, results in disastrous debris flows causing more hazards [2]. Therefore, it is necessary to evaluate the risk caused by rock fall in order to protect residential areas and foundations. Rock fall susceptibility mapping means partitioning a region into homogeneous zones and ranking these zones based on the actual or potential risk of a mass movement on their slopes [3]. Rock fall susceptibility mapping helps designers and engineers choose the right location for the development projects; so, its results can be utilized in instability management and land use designing [4]. A wide range of models have been developed for rock fall evaluation and they differ in terms of complexity, processes considered, and data required for model calibration and model use. They are divided into three main classes including 1) empirical models [5], 2) process-based models for describing or simulating the types of rock movements over the surface of slopes [6], and 3) GIS-based models running within a GIS workspace or raster-based

\*Corresponding author's email: mokhtari@yazd.ac.ir

models for which the input data are prepared using the GIS software [7]. There have been few attempts on mapping rock-fall susceptibility by means of GIS [7]. Also, due to warning systems, limitation in implementation, cost, and time-consuming, it is necessary to integrate remote sensing and Geographic Information Systems (GIS) in rock fall models to obtain important information in identifying and assessing of rock fall risk susceptibility maps. This has been proven to be of great help in the assessment, management, and mitigation of mass movements in susceptible areas where civil projects are running or where mining activities could increase the risk of rock fall [8]. In areas in which mining activities are in progress, ground vibration could contribute to the existing factors so rock fall susceptibility maps can help to have plans for areas prone for this issue. Such maps are of great use for civil projects as well.

Several approaches including inventory- based methods/ or heuristic analysis, and semi- quantitative and quantitative techniques have been developed for Landslide and rock fall susceptibility mapping [9, 10]. Inventory- based methods involve the collection of past landslide records, construction of databases, and creation of susceptibility maps based on those data [11, 12]. Heuristic analysis consists of geomorphologic analyses, where researchers directly determine susceptibility. This method is used by geomorphologists to analyze aerial



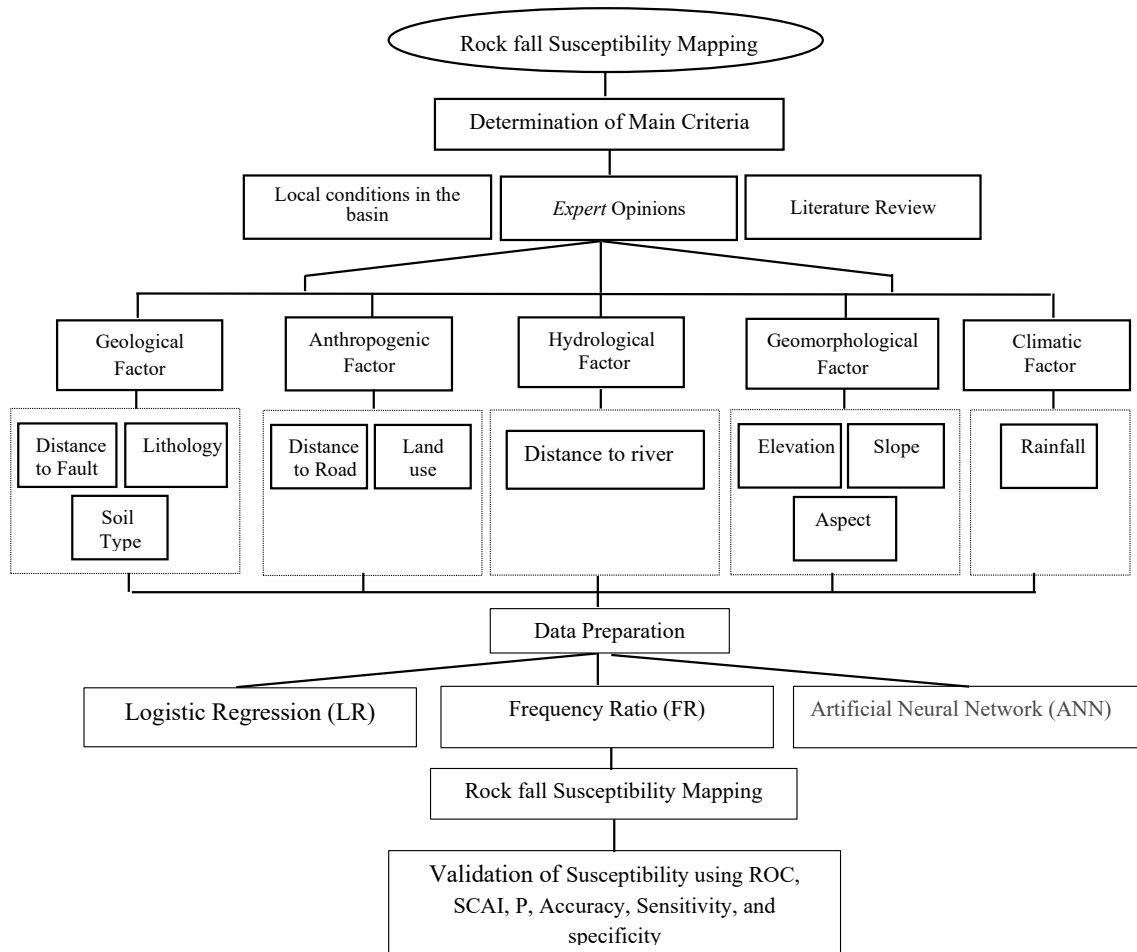


Fig. 1 Schematic flowchart of the methodology

photographs or to conduct field surveys [13-15]. The semi-quantitative method is a combination of qualitative methods in which the analyst uses his expert knowledge to weight the factors affecting landslide and rock fall susceptibility. Notable among these methods are the Analytic Hierarchy Process (AHP) [16, 17], and the Weighted Linear Combination (WLC) [16, 18]. Because of their empirical nature, these methods are each specific to certain regions, climates, and vegetation types [19]. Therefore, they need to be modified and re-verified before they are used in other areas. In these methods, landslide factors are weighted based on experts' experience and knowledge. Thus, some parameters may have greater effects on the zoning results than others, but these weights may vary depending on the characteristics of the area [20].

Quantitative methods such as statistical, machine learning models, and deterministic approaches can be employed [10, 21]. A statistical method determines and analyzes the factors affecting landslide and rock fall based on similarity (in terms of environmental conditions) to the areas where they have already occurred. In this method, landslide probability is a function of the presence and roles of independent variables including inherent and environmental factors. Statistical techniques require the collection of large amounts of data to produce reliable results. This method can be implemented as

a bivariate statistical model [22] or a multivariate statistical model [23, 24]. Notable bivariate models include Information Value (IV) [25], Certainty Factor (CF) [26, 27], Weights of Evidence (WOE) [17, 28, 29], logistic regression [30, 31], and frequency ratio [10, 17]. Given the complexity of landslide prediction, in recent years, there has also been an increased use of machine learning methods including fuzzy methods [32, 33], neural networks [34, 35], support vector regression [36, 37], and neuro-fuzzy methods [38, 39]. Mechanical approaches also facilitate the assessment and analysis of slope stability by using deterministic methods (e.g., the limit equilibrium method) or numerical methods (e.g., continuous or alternative modeling). A review of the technical literature shows that this approach has been successfully used many times for landslide and rock fall risk analysis [40, 41]. However, these methods need exhaustive data for each individual slope. They are, therefore, only suitable for small-scale mapping. Identifying areas prone to rock fall is one of the primary measures in managing natural resources and reducing the damage caused by this phenomenon. Avoiding this phenomenon is possible when there is a good understanding; one the one hand, slopes instability in the framework should be investigated to prepare the zoning map of rock fall and recognize areas with a high potential risk within the scope of human activities; on the other hand, safe

locations for the development of residential areas and other future uses are considered as an essential matter in reducing damages and achieving sustainable development. This study was aimed to evaluate and compare the results of rock fall susceptibility maps using three models, i.e., frequency ratio, regression logistic, and neural network models, for the rock fall susceptibility assessment of a semi-mountainous region facing active rock falls. For this purpose, nine maps representing slope, lithology, land use, slope aspect, rainfall, distance to road, distance to fault, distance to stream and elevation were employed for rock fall susceptibility mapping. The susceptibility maps constructed by each model were analyzed based on the area under the curve (AUC) values of relative operating characteristic (ROC) curves, seed cell area, the P index, Accuracy, Sensitivity, and specificity. The flowchart in Fig. 1 shows the schematic representation of the rock fall susceptibility maps developed in the study area.

## 2. GEOLOGICAL SETTING

The study area is situated in Yazd Province, a central region in Iran. The area of Taft County (Fig. 1) is 5580-km<sup>2</sup>, between the latitudes of 31° 99' to 31° 30' N and the longitudes of 53° 57' to 54° 56' E. The annual precipitation is 186 mm. Based on A-pan evaporation measurements, cumulative potential evaporation reaches 2395 mm annually. The average annual temperature is 14 °C, while the minimum and maximum temperatures are 6.3 °C and 21.7 °C, respectively. This area is located in an arid and semiarid part of Iran. In terms of topography, the study area lies within an east-west valley bounded by limestone units in the north and Shirkouh heights in the south. The southern and north-eastern parts of the area have a flat terrain, and its edges are covered by a chain of low hills. The mountainous parts are intermittently interrupted by small plains. The study area comprises five different lithological units including: very hard rock units (Granite and basalt volcanic), hard rock units (Dolomite with sandstone, dense yellow dolomite, alternation of dolomite, and reef type limestone), Medium rock units (Marl and limestone, grey shale and sandstone), weak rock units (Gypsiferous marl, shale, shale and fossiliferous limestone), and very weak rock units (Low level pediment fan and valley terrace deposits). A survey showed that the study area had the highest frequency of rock fall events within Yazd province. Fig. (2) shows an image of a rock fall occurring in a rural part of the study area and the resulting damages. The existence of residential areas on sharp slopes, human activities there, and low-resistance rock formations have led to instability and slides.

## 3. DATABASE AND METHODOLOGY

### 3.1 Data Preparation

To prepare the rock fall susceptibility map, a map of the rock fall distribution was required. For this purpose, aerial photos of the region with block number 282 at a scale of 1: 20000 were interpreted by stereoscopy approach and the areas suspicious of rock fall were determined. Then, the location of the rocks was recorded through field surveys using the global positioning system (GPS); finally, 620 rock falls were

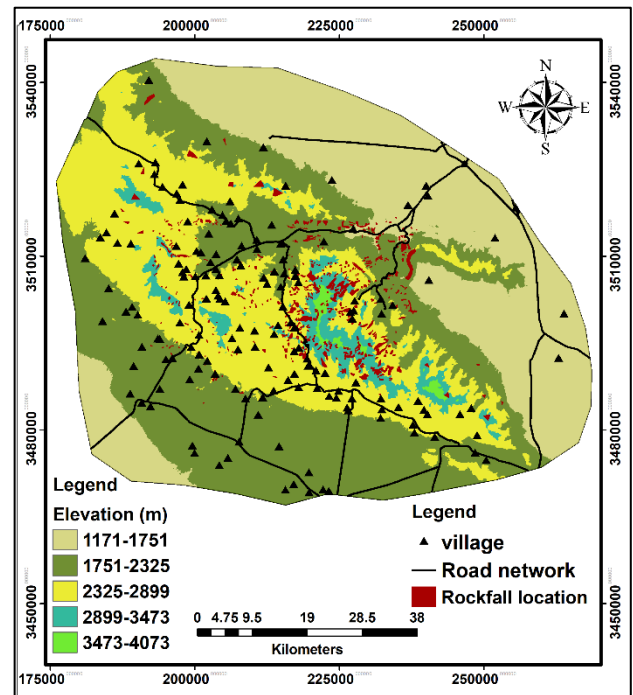


Fig. 2 Location map of the study area

recorded. All these steps were executed by the office of natural resources and water management of Yazd Province. Rock falls covered about 62.67 km<sup>2</sup> of the study area. The area of the smallest and largest landslides was about 0.0046 km<sup>2</sup> and 3.22 km<sup>2</sup>, respectively. The rock fall locations were partitioned into training data set 70% (434 rock fall locations) and a testing data set 30% (186 rock fall locations) and similar proportions for non-rock fall category in testing and training. The influential factors on rock fall were characterized in this research based on regional condition, available data, and the factors employed in literature [17, 42] in this context. The factors included slope angle, slope aspect, elevation, distance from faults, rainfall, distance from roads, distance from streams, land use, and lithology (Fig. 3). For mapping the landslide-susceptible areas based on the mentioned criteria, the data related to each individual criterion must initially be transformed into a layer in the GIS software. The procedure followed in this regard is described below.

**Slope** : slope is one of the main parameters that increase the rupture potential of hillsides. In this regard, it serves as a stimulating factor. Any increase in the hillside slope can cause an increase in the weight force along the slope. Whenever the increase exceeds the vertical weight force, a landslide occurs [43]. In this study, the Raster Surface tool was used in the ArcGIS software to extract a Slope map from a digital elevation model map. The extraction was in terms of percentages, and, based on the equivalence interval classification method, the map was categorized into five classes with 10% intervals. **Aspect**: the aspect of hillside is a determining factor in the occurrence of mass motions. In the northern and western hillsides, due to the high humidity, the occurrence of landslide is frequent. In the eastern and southern hillsides, however, due to maximal absorption of energy and minimal



Fig. 3. Examples of rock falls inside the study area: (a) Abdullah village; (b) over the road in Taft country

amount of water remaining in the soil, mass motions are very infrequent[44]. In this case, the Raster Surface tool was used in the ArcGIS software to extract an Aspect map from a digital elevation model map. The extracted map was then classified into five plane surfaces including ( $0^{\circ}$  -  $10^{\circ}$ ), northern ( $10^{\circ}$ - $45^{\circ}$ ,  $315^{\circ}$ - $360^{\circ}$ ), eastern ( $45^{\circ}$ - $135^{\circ}$ ), southern ( $135^{\circ}$ - $252^{\circ}$ ) and western ( $225^{\circ}$ - $315^{\circ}$ ) surfaces.

*Distance to fault:* when landslides occur, faults can play the role of intensifiers that affect the hillsides in various ways. Among the impacts, one may refer to crushing and brecciation in the fault zone, penetration of water from this area into the hillsides, disruptions around the fault, and different rates of erosion in the hillsides[45]. In this research, faults of the region were extracted from a geological map on the scale of 1: 100,000. Then, using the Distance tool in the ArcGIS software, a map of fault distances was prepared and categorized into six classes with 500m intervals.

*Rainfall:* another factor that plays a role in the occurrence of landslides is the penetration of rain water into hillsides. This leads to increased pore pressure, decreased soil sucking, increased unit weight of the soil, and, as a result, reduced shear strength of the soil. These factors join hands to make hillsides prone to landslides[46]. The effectiveness threshold of the factors depends on the characteristics of the area. In this study, according to the statistics provided by Yazd province weather station and by using the Inverse Distance Weighting (IDW) statistical technique, a rainfall raster layer was interpolated as an annual iso-precipitation map with iso-precipitation curves. It was finally categorized into three classes.

*Lithology:* Different rocks have different degrees of resistance to external forces. This is due to the difference in their sediment composition as well as the geological period and conditions in which they were formed[47]. In this respect, a petrology paper map of the study area on the scale of 1: 100000 was received from the Geological Survey Department of Iran. Then, the lithological features of the catchment were extracted by the ArcGIS software. According to those features, the rocks were classified into five categories including very hard, hard, medium, weak, and very weak rocks.

*Distance to stream:* the impact of stream is observed as a set of external dynamic functions and mechanical activities. In this

case, one can refer to such impacts as saturation of materials, increase in mass volume, decrease in the mechanical strength of soil and rock masses, rise in underground water Tables and increase of static and dynamic loads[48]. A stream map was extracted from a topographic map of the catchment on the scale of 1: 50000. Then, using the Distance tool in the ArcGIS software, a map of stream distances was prepared and classified into five categories with 300m intervals.

*Distance to road:* Among human activities, road construction has the most important role in the occurrence of new landslides and stimulation of old ones. Road construction leads to increased pore pressure, increased weight of the soil mass, and reduced adhesion. It all occurs due to the reduction of the slope length, increase of the gradient, and the lack of suitable drainage to discharge the extra underground water during the road construction process[49]. In order to prepare a map of distances to roads, the road network was extracted from a 1: 50000 digitized topographic map of the catchment. Then, using the Distance tool in the ArcGIS software, the map of distance to road was prepared and classified into 5 classes with 300 m intervals. *Land use* is one of the most important features to take into account in the analysis and risk zonation of slope stability. Since vegetation has a significant impact on preservation of soil and reduction of erosion, areas with denser vegetation are less susceptible to landslides[50]. In order to map the land use ever practiced, a land use map of the basin on the scale of 1:100,000 was adopted from the Iranian Forest, Rangeland, and Watershed Management Organization (FRWO). Then, based on the type of land use, the layer was categorized into six classes of farmland, poor vegetation, moderate vegetation, good vegetation, bare land, and residential areas. *Elevation*, as a parameter of indirect effects, is a determinant of many factors that cause landslides, such as annual precipitation, distribution of vegetation, physical degradation and chemical weathering[51]. In this research, the Triangular Irregular Network (TIN) model was used to generate a Digital Elevation Model (DEM) for the study area from digitized lines with the resolution of  $20 \times 20$  m-pixels. Then, the digital elevation model map was divided into five classes with intervals of 574 m. Causative factors, scales,

**Table 1. Causative factors, scales, and classes**

Causative factor	Classes	GIS data type	Scale or resolution
Slope (%)	Less than or equal to 10 10 to 20 20 to 30 30 to 40 Greater than 40	Grid	20 m×20 m
Slope aspect	Flat North East South West	Grid	20 m×20 m
Elevation (m)	1177-1751 1751-2325 2325-2899 2899-3473 3473-4047	Grid	20 m×20 m
Land use	Farmland Poor pasture Moderate pasture Good pasture Bare land Residential area	Polygon converge	1:100,000
Distance to road (m)	<300 300-600 600-900 900-1200 >1200	Line converge	1:100,000
Distance to fault (m)	<500 500-1000 1000-1500 1500-2000 2000-2500 >2000	Line converge	1:100,000
Distance to stream (m)	<300 300-600 600-900 900-1200 >1200	Line converge	1:100,000
Rainfall (mm)	9-13 13-18 18-26	Grid	20 m×20 m
Lithology	Very hard rock Hard rock Medium rock Weak rock Very weak rock	Polygon converge	1:100,000

classes, and data type are presented in Table 1.

### 3.2. Multicollinearity analysis of landslide conditioning factors

In preparing a landslide susceptibility map, it is necessary to investigate the correlation between the factors affecting a landslide. Tolerance (TOL) and variance inflation factor (VIF) are two indices that are widely used to investigate the correlation. Tols smaller than 0.1 and VIFs greater than 10

indicate high correlations[52]. In this research, the correlation between the input parameters was investigated, whose results are presented in Table 2. As the results show, there is no correlation among the 13 factors affecting the landslide.

### 3.3. Methodology

#### 3.3.1. Artificial Neural Network

Artificial neural networks (ANNs) are data- driven and flexible computing models and general non-linear functional

**Table 2. Multicollinearity analysis of landslide conditioning factors**

No.	Landslide conditioning factor	TOL	VIF
1	land use	0.944	1.059
2	lithology	0.812	1.232
3	precipitation	0.735	1.360
4	slope degree	0.801	1.249
5	slope aspect	0.910	1.099
6	elevation	0.946	1.057
7	distance to fault	0.828	1.208
8	distance to stream	0.903	1.107
9	distance to road	0.877	1.141

approximation approach. As a result, ANNs are considered as significant modeling methods for landslide or rock fall susceptibility zonation [53]. The capability of ANNs to learn non-linear functions from the data is a significant characteristic in the case of sorting rock fall-prone districts. The problem of partitioning a land area into landslide susceptibility zones can be presented as a classification problem. In this problem, the output of an ANN is the degree of the membership of each terrain unit with regard to each landslide susceptibility class. The higher the degree of membership is, the greater the landslide susceptibility of the terrain unit will be, and vice versa [54].

Different ANN models are distinguished by their three integral characteristics, namely transfer function, network architecture and learning rules. Every neural network works in three phases including learning, generalization, and operation. Multi-Layer Perceptron (MLP) is among the most popular and widely used variants of artificial neural networks. This network consists of an input layer, an output layer, and one or more hidden layers between these two (Fig. 4). The task of hidden layers is to enhance the ability of the network to model complex functions [55]. The number of neurons in the first layer depends on the number of model parameters (nine in this study), and the output layer neurons are as many as the outputs of the landslide prediction (as considered in this study). The optimal number of hidden layers can be determined by trial and error. Each layer of this network contains multiple neurons, the number of which varies depending on the application. Each neuron receives one or more inputs, which it processes using a transfer function (linear, sigmoid, logistic-sigmoid) to produce an output signal. The signal is then sent to subsequent neurons. The mentioned processing in a typical neuron consists of multiplying each input by a corresponding weight, summing the answer with a value known as bias, and using the result as the input of the transfer function to produce the output signal.

The most important step in developing a neural network is

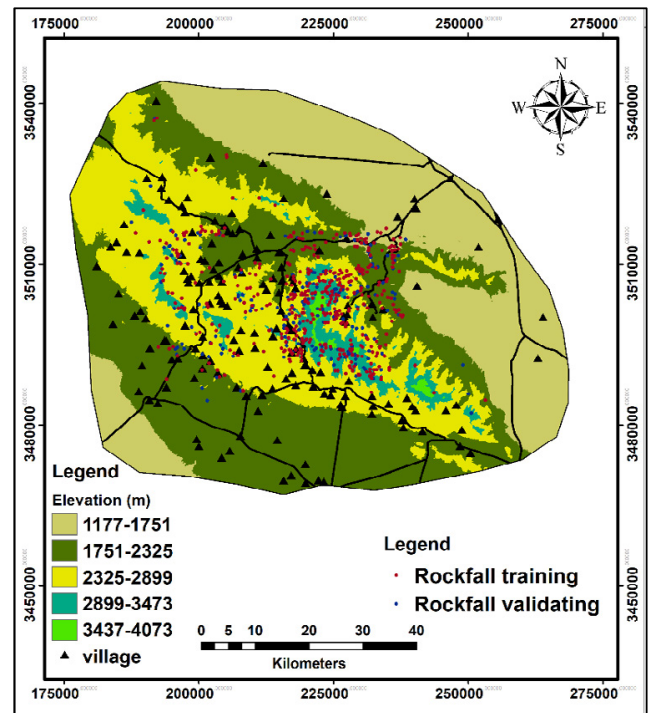


**Fig. 4. Distribution of training dataset in the study area**

learning (also known as training). The neural network can be trained through several methods, the most notable of which is the error back propagation algorithm. The MLP was trained by the back propagation algorithm and then adopted in this study. As a common practice, the data were divided into two sets: training and test. The training dataset covered two subsets of rock fall prone areas and non-rock fall prone areas. The cells to be used for network training were randomly chosen from both subsets. In each class, 70% of the data were used for network training and calibration, and the remaining 30% were reserved for testing. Data normalization is a common standard data pre-process in developing ANN models. It is

suggested that every parameter should be linearly scaled to the range of [0.1, 0.9], [-1, +1] or [0, 1]. In the modeling of this study, the following equation was used to scale the data sets of all the input variables to the interval [0.1, 0.9]:

$$N_i = 0.8 \left( \frac{X_i - X_{\min}}{X_{\max} - X_{\min}} \right) + 0.1 \quad (1)$$

Where  $N_i$  is the normalized value,  $X_i$  is the original data,  $X_{\min}$  and  $X_{\max}$  are the minimum value and the maximum value of original data, respectively [56]. As it is commonly done for network training, the models and parameters were formulated such that the Root Mean Squared Error (RMSE) would be minimized. After the network goal was reached, the study area was fed into the network to assess rock fall susceptibility (Fig 6b).

### 3.3.2. Frequency Ratio

The frequency ratio method is a bivariate statistical method highly recommended for estimating landslide susceptibility based on the observed relationship between landslide distribution and each of its causative factors. This method can be used to establish a spatial correlation between a landslide location and its explanatory factors [57]. To determine the frequency ratio, the number of rock fall pixels in each class has been evaluated and the frequency ratio for each factor class is calculated by dividing the rock fall ratio by the area ratio, denoted as [58]:

$$FR_{i,j} = \frac{Npix(S_{i,j}) / \sum_j Npix(S_{i,j})}{Npix(N_{i,j}) / \sum_j Npix(N_{i,j})} \quad (2)$$

Where  $FR_{i,j}$  is the frequency ratio of class  $j$  in factor  $i$ ;  $Npix(S_{i,j})$  is the number of pixels of rock fall occurrence within class  $j$  in factor  $i$ ;  $Npix(N_{i,j})$  is the number of pixels of class  $j$  in factor  $i$ . FR values of greater than 1 signify a strong relationship between the rock fall event and the factor, FR values of 1 represent a moderate correlation, and FR values of less than 1 indicate a weak relationship between the two [57]. The rock fall susceptibility index (RSI) was calculated by the following equation:

$$RSI = \sum FR_{i,j} \quad (3)$$

where RSI is the rock fall susceptibility index, and  $\sum FR_{i,j}$  is the sum of the sub-class of effective factor values. To obtain RSI, the layers of nine factors used in the FR method were converted into a grid format. Then, each factor was divided into several classes (Table 1), and the reclassified layers are intersected in the rock fall event layer. Next, the number of rock falls in each class of each factor and the corresponding percentages were obtained. Finally, RSI was calculated by summing the frequency ratios of each factor. RSI represents the relative chance of rock fall occurrence, and its higher

values indicate a higher risk of rock fall.

### 3.3.3. Logistic Regression

Logistic regression is a multivariate analytical method from the family of generalized linear statistical models. The main goal of logistic regression is to model the occurrence probability of a conventional two-state event, the presence/absence of different factors, and the significance of this presence/absence [59]. In the present study, the logistic regression model was used to analyze the spatial association between the rock fall event and its causative factors. The goal was to find the best model for explaining the relationships between the occurrence/non-occurrence of the dependent variable (rock fall event) and a set of independent variables affecting the rock fall occurrence. The relationship between an occurrence and its dependency on several variables can be quantitatively expressed using the following equation [60]:

$$P = \frac{1}{(1 + e^{-Z})} \quad (4)$$

where P is the probability of occurrence of the event, and Z is a linear parameter defined as follows:

$$Z = C_0 + C_1 X_1 + C_2 X_2 + \dots + C_n X_n \quad (5)$$

where Z is the the dependent variable representing the presence of rock fall (1) or absence of rock fall (0), y-intercept of the model,  $C_1, C_2, \dots, C_n$  denotes the coefficients of the logistic regression model, and  $X_1, X_2, \dots, X_n$  denotes the independent factors of the model. As Z changes from  $+\infty$  to  $-\infty$ , rock fall probability varies on an S-shaped curve from 0 to 1. The higher this value is, the greater the likelihood of a rock fall will be. Conversely, the closer the value is to zero, the less likely the chance of this event will be [60]. To develop a logistic regression model, the rock fall event distribution layer and the layers of nine determinant factors were reclassified and standardized by scaling to the 0-1 interval. All the layers were then converted from a raster format into an ASCII format.

### 5.2. Statistical measures

In order to investigate the performance of landslide models, three statistical evaluation measures including Accuracy, Sensitivity and Specificity were used[36]. Sensitivity is the portion of landslide pixels correctly classified as landslides, indicating the predicting capability of the model to classify landslides. Specificity is the portion of non-landslide pixels properly classified as non-landslides, indicating the predicting capability of the model to classify non-landslide pixels. Accuracy is the portion of correctly-classified landslide and non-landslide pixels, representing how well the model performs. They can be calculated using the following equations:

$$Sensitivity = \frac{TP}{TP + FN} \quad (6)$$

$$Specificity = \frac{TN}{TN + FP} \quad (7)$$

$$Accuracy = \frac{TP + TN}{TP + TN + FP + FN} \quad (8)$$

where TP (true positive) and TN (true negative) represent the number of landslide pixels and non-landslide pixels that are properly classified, respectively. FP (false positive) and FN (false negative) indicate the number of landslide pixels and non- landslide pixels that are incorrectly classified.

## 4. RESULTS AND DISCUSSIONS

### 4.1. Rock fall susceptibility assessment by ANN

A three-layer feed-forward network consisting of an input layer (nine neurons), one hidden layer (7 neurons) and one output layer was used as a network structure of 9-7-1. At the end of training the developed network, its RMSE values for training and test sets declined to 0.0145 and 0.0173, respectively. Rock fall and non-rock fall points and the data of the effective parameters at those points were extracted as a text file by using the IDRISI software with the statistical format of the STATISTICA software. Then, the text file was transferred into MATLAB using an appropriate format of STATISTICA. In the MATLAB workspace, neural networks were implemented on the text file data, and the obtained neural network was stored for running on all of the region's data. Also, all of the effective factors in all the intra-border cells were transferred into MATLAB in the same procedure. Then, an appropriate neural network generated and stored by means of the training and test data in the MATLAB was run on the data of the whole area. The obtained result, which was non-mapping, was transferred back from MATLAB into STATISTICA and then into IDRISI. Through the transfer of the STATISTICA text data into IDRISI, the non-map text data were converted into a raster map. To obtain the rock fall susceptibility map, the RSI needed to be reclassified into several different susceptibility classes. The authors considered several classification methods that could be used for this purpose, including quantiles, natural breaks, equal intervals, and standard deviations [18]. In general, choosing the classification method depends on the histogram of landslide susceptibility indices. After reviewing the options, the natural break classification scheme was used to classify the RSI into three classes: low, moderate, and high. The rock fall susceptibility map obtained by using the developed ANN model is illustrated in Fig (5a). As the map shows, 12.3% of the study area belongs to the high-susceptibility class, 10.7% of the total area belongs to the moderate-susceptibility class, and the remaining 77% belongs to the low-susceptibility class.

### 4.2. Rock fall susceptibility assessment by FR

The FRs calculated by the probability model for the rock fall susceptibility factors are presented in Table (2). The Table

shows the relationship between landslide occurrence and each factor. In the case of slope angle, the angles greater than 20 percent correspond to FRs greater than 1, and the highest ratio, which represents a high probability of rock fall, belongs to the slopes steeper than 40 percent. The results also show that the slopes with an eastern-western aspect have the highest rock fall frequency. In terms of land use, the highest rock fall frequency is observed in a good pasture. Regarding the relationship between elevation and rock fall occurrence, the highest rock fall frequency can be observed in the elevation range of 2899-3473 m. Furthermore, the areas at the distance of 900-1200 m from roads have the highest FR and, therefore, the highest probability of rock fall.

An examination of the relationship between rock fall occurrence and the distance from faults indicated that rock fall probability is the highest within the distance of 500 m from faults. However, as this distance increases, there is a decrease in the FR and, thus, in the probability of rock fall. Considering rainfall, the highest rock fall frequencies belong to areas with the rainfall of 13-18 mm, and then to areas with the rainfall of 9-13 mm. Studying lithology, as a determinant of rock fall susceptibility, showed that the highest FR belongs to the very hard rock and the lowest probability belongs to the very weak rock including alluvial materials. This can be attributed to the slope angle of sedimentary units covering areas with less than 5% slope resulting in infrequent occurrence of rock fall. The FR model as a simple bivariate method for predicting rockfalls. A major advantage of the FR model is its ability to explore the correlation between a landslide location and the class of individual factors that significantly affect the rockfall occurrence. However, it has an important limitation; as a bivariate model, it is not capable of determining the weights of input factors. The rock fall susceptibility map obtained by using the developed FR model is illustrated in Fig (5b). In this map, high-susceptibility, moderate-susceptibility, and low-susceptibility zones constitute 10.47%, 24.61%, and 64.92% of the total area, respectively.

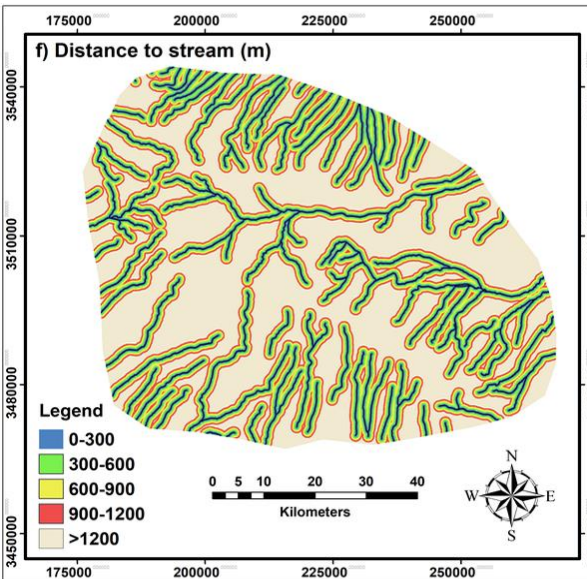
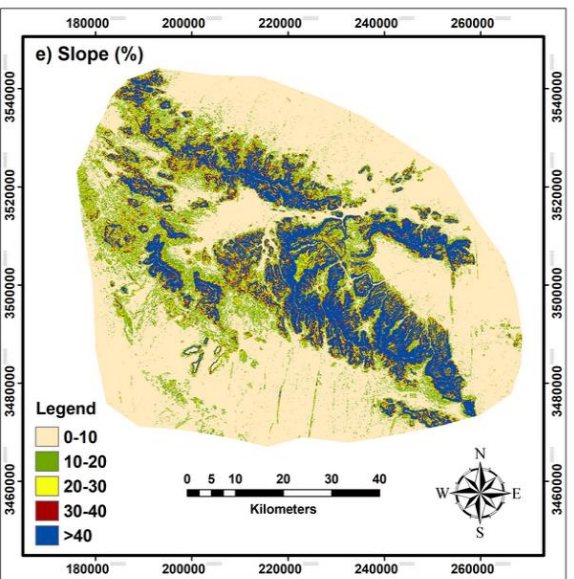
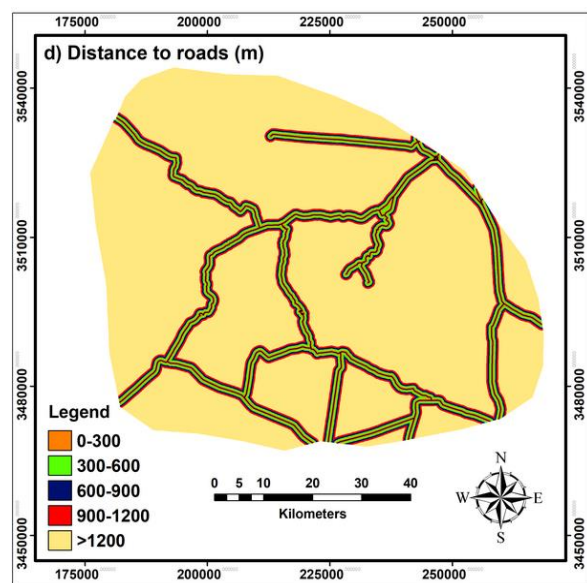
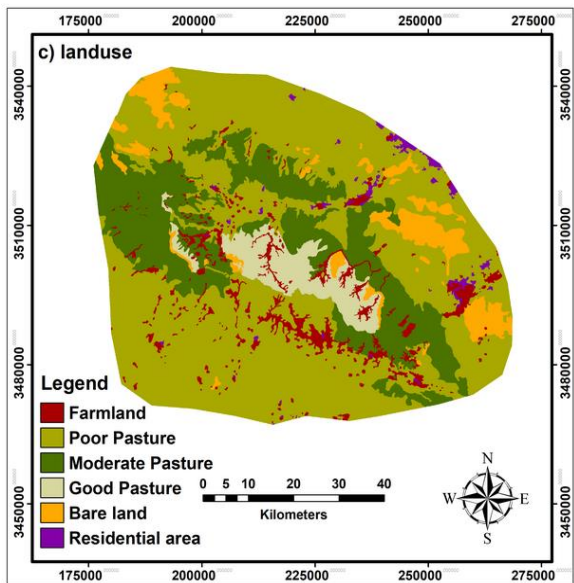
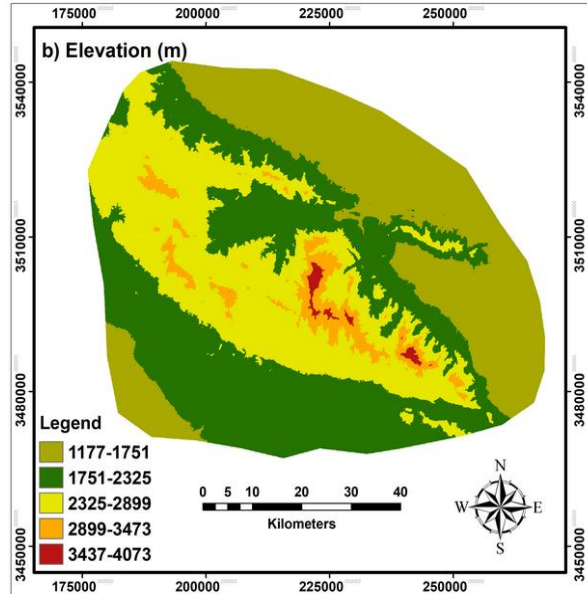
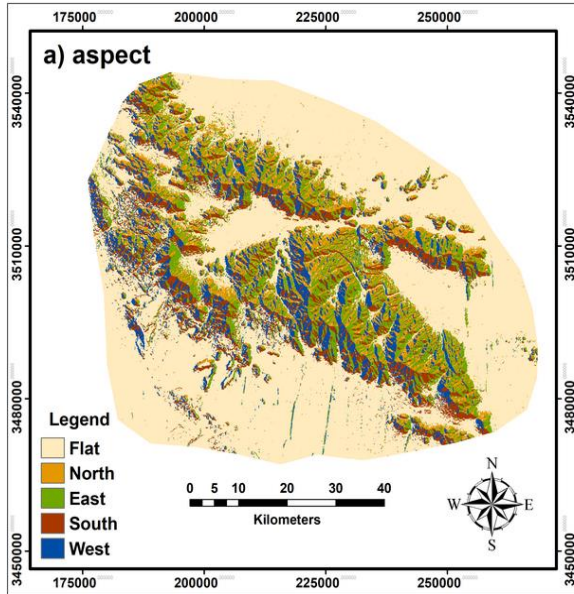
### 4.3. Rock fall susceptibility assessment by LR

Prior to the logistic regression analysis, all the layers (i.e., the rock fall event distribution layer and the layers of the nine factors) were converted from a raster format to an ASCII format. The results of the logistic regression are provided in Table (3).

The regression coefficients listed in Table (3) were inserted into Eq. (4), and the following linear relationship was obtained accordingly:

$$Z = -5.6479 + 1.6852 \text{ Slope} + 0.2375 \text{ Aspect} + 3.1448 \text{ Elevation} + 0.4925 \text{ Fault} - 1.4759 \text{ Lithology} - 1.3720 \text{ Landuse} - 1.3348 \text{ Rain} + 0.0867 \text{ Stream} + 1.089 \text{ Road} \quad (9)$$

After substituting the above relationship in Eq. (3), the final equation of logistic regression was obtained as



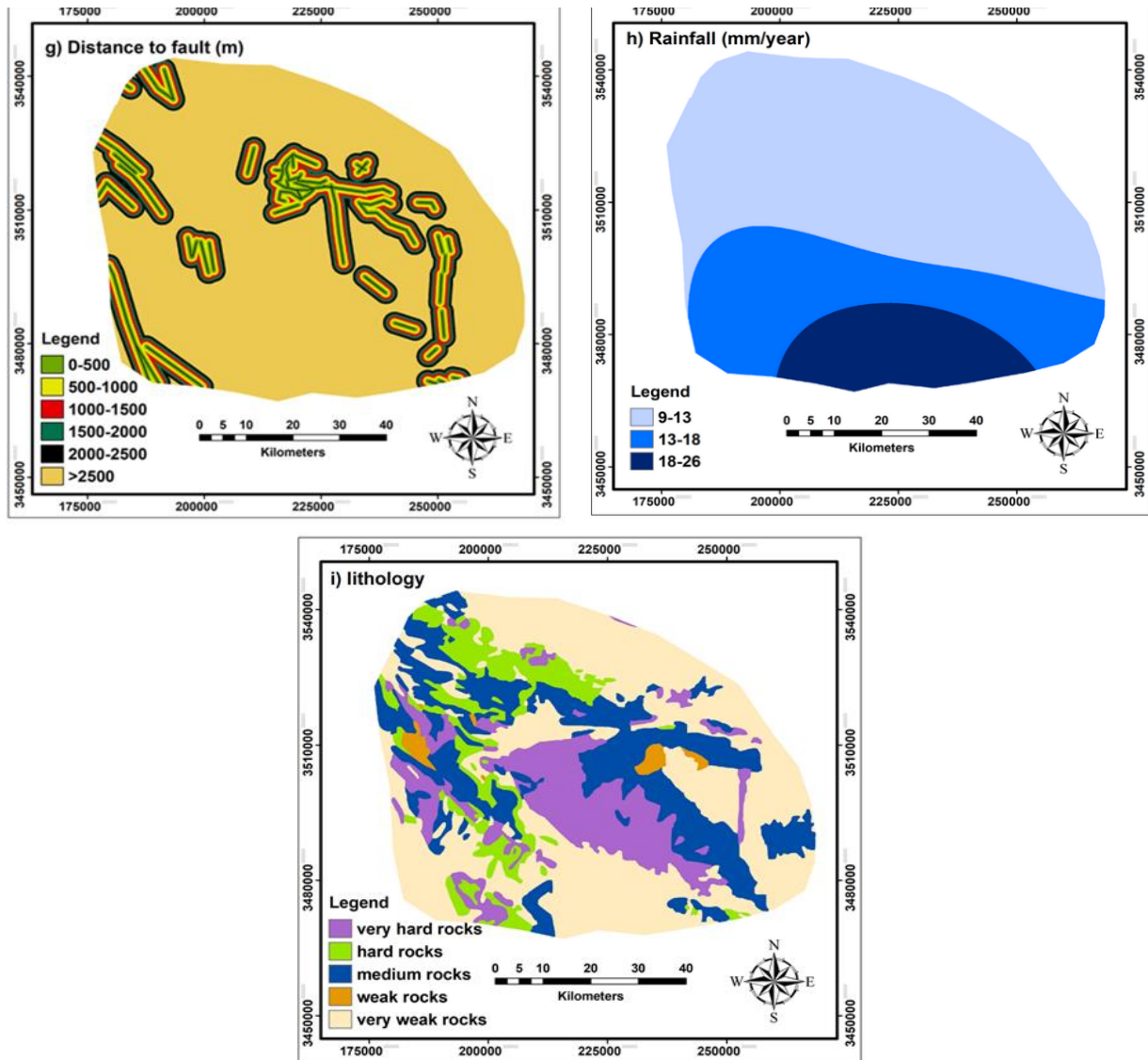


Fig. 5. Effective factors on rock fall occurrence in the study area, including: (a) aspect; (b) elevation; (c) land use; (d) distance to road; (e). slope; (f) distance to river; (g) distance to fault; (h) rainfall; and (i) lithology

follows:

$$P_{(Rockfall\ occurrence)} = \frac{1}{1 + e^{-(5.6479 + 1.6852\ Slope + 0.2375\ Aspect + 3.1448\ Elevation + 0.4925\ Fault - 1.4759\ Lithology - 1.3720\ Landuse - 1.3348\ Rain + 0.0867\ Stream + 1.089\ Road)}} \quad (10)$$

In Eq. (6), the coefficients of slope, aspect, elevation, distance from faults, distance from roads, and distance from streams are positive, indicating that the mentioned factors have a positive relationship with rock fall probability. On the contrary, the coefficients of lithology, land use, and rainfall were negative, which signifies their inverse relationship with the probability of rock fall in the study area. Finally, a susceptibility map was obtained by converting the file into a

raster format (Fig. 5c). In the map obtained by this approach, high-susceptibility, moderate-susceptibility, and low-susceptibility zones cover 8.26%, 23.04%, and 68.70% of the total area, respectively.

#### 4.4. Landslide susceptibility maps

The landslide susceptibility maps are classified into different susceptibility categories to visually interpret. Many data clustering approaches proposed to determine the optimal arrangement of values into different classes including quantiles, natural breaks, equal intervals, and standard deviation[61]. Overall, choosing the appropriate classification approaches relies on the distribution of landslide susceptibility values[61]. As an example, equal interval or standard deviation approaches can be applied when data distribution is about normal. When data are positively or negatively skewed, the quantile or natural break methods can be used

**Table 2. Result of the frequency ratio for each factor**

Caused factor	Classes	No. of pixels in domain	Percent of domain	No. of rock fall	Percent of rock fall	FR
Slope%	≤10	7994001	57.3	9786	6.05	0.105
	11-20	1921617	13.8	21402	13.22	0.95
	21-30	1103671	7.91	25195	15.56	1.96
	31-40	843902	6.04	24368	15.05	2.49
	≥40	2086497	14.95	81124	50.12	3.35
Slope aspect	Flat	8194054	58.74	14629	9.04	0.15
	North	1407228	10.1	35274	21.8	2.15
	Earth	1594830	11.43	44542	27.5	2.40
	South	1392946	9.98	30455	18.80	1.88
	West	1360630	9.75	36975	22.86	2.34
Land use	Farmland	745015	5.34	6722	4.15	0.77
	Poor pasture	8314089	59.60	43369	26.81	0.45
	Moderate pasture	3050423	21.86	52266	32.28	1.47
	Good pasture	758822	5.44	55970	34.57	6.35
	Bare land	941639	6.75	3432	2.12	0.31
	Residential area	139700	1.01	116	0.07	0.07
Elevation(m)	1177-1751	4223876	30.27	5572	3.44	0.11
	1751-2325	5139824	36.84	36514	22.56	0.61
	2325-2899	3930787	28.20	67817	41.90	1.48
	2899-3473	588860	4.22	48002	29.65	7.02
	3473-4047	66341	0.47	3970	2.45	5.22
	>500	10260665	73.55	107049	66.13	0.89
Distance to fault (m)	<500	827495	5.94	19416	11.99	2.01
	500-1000	748434	5.36	11276	6.96	1.30
	1000-1500	712744	5.12	10342	6.40	1.25
	1500-2000	703576	5.04	7218	4.46	0.89
	2000-2500	696774	4.99	6574	4.06	0.81
	>2500	10260665	73.55	107049	66.13	0.89
Distance to stream (m)	<300	2114301	15.15	17037	10.52	0.69
	300-600	2011119	14.42	14136	8.73	0.60
	600-900	1900697	13.63	14794	9.14	0.67
	900-1200	1613301	11.56	18878	11.66	1.01
	>1200	6310270	45.24	97030	59.95	1.32
Rainfall (mm)	9-13	8164557	58.53	107573	66.46	1.13
	13-18	3870982	27.75	54302	33.54	1.21
	18-26	1914149	13.72	0	0	0
Lithology	Very hard rock	2331457	16.71	77126	47.65	2.85
	Hard rock	1425552	10.21	4205	2.59	0.25
	Medium rock	3443780	24.69	69532	42.95	1.73
	Weak rock	187851	1.35	3885	2.40	1.77
	Very weak rock	6561048	47.04	7127	4.41	0.09
Distance to road (m)	<300	689191	4.94	6118	3.78	0.76
	300-600	639421	4.58	5976	3.70	0.81
	600-900	618361	4.43	7858	4.85	1.09
	900-1200	596808	4.28	7887	4.87	1.13
	>1200	11405907	81.77	134036	82.8	1.01

for classification[48]. In the present study, the quantile and natural break classifiers were applied to the data based on their distribution histogram. The visual comparison between the obtained results revealed that the natural break classification method provides better results than the quantile method does. Accordingly, the natural break technique was employed,

and low-, moderate-, and high-susceptibility categories were considered in providing landslide susceptibility index maps. Fig. 7a-g presents the landslide susceptibility maps.

#### 4.5. Validation of rock fall susceptibility maps

The rock fall susceptibility zoning performance of the

**Table 3. Coefficients of logistic regression**

Caused factor	Coefficients of logistic regression	Mean	Standard Deviation
Slope	1.6852	0.3538	0.3401
Slope aspect	0.2375	0.3495	0.3344
Land use	-1.3720	0.5488	0.1850
Elevation	3.1448	0.3852	0.2163
Distance to road	1.098	0.1222	0.2802
Distance to fault	0.4925	0.1524	0.2999
Distance to stream	0.0867	0.3728	0.3848
Rainfall	-1.3348	0.3586	0.3330
Lithology	-1.4759	0.6823	0.3399

methods used was evaluated by using a Receiver Operating Characteristic (ROC) curve. To draw an ROC curve, a true positive rate (sensitivity) must be plotted against a false positive rate (1- specificity). The area under the ROC curve ranges from 0.5 to 1; in fact, the closer it is to 1, the better the performance of the method [62]. To plot a ROC curve and calculate the area under the curve (AUC), for different thresholds ranging from 0 to 1, we determined the number of cells in which rock fall occurrence was correctly and incorrectly predicted, as compared to the observed data. The true positive and false positive rates were then calculated accordingly. These two rates were then sorted in an ascending order and plotted to obtain the ROC curve. Fig. (8) shows the ROC curves, and Table (4) presents the results obtained for each method. As shown, the AUCs of the LR, ANN, and FR models were found to be 0.833, 0.893 and 0.899, respectively. Thus, the FR and ANN methods outperformed the LR method in the studied area. By considering the ROC curve, the AUC between 0.9 and 1 could signify the excellent performance of the model, and the AUC between 0.8 and 0.9 would represent the good performance of the model. On the other hand, the AUCs of 0.7-0.8, 0.6-0.7 and 0.5-0.6 could show the average, bad, and very bad performance of the model, respectively [63]. According to this classification, all of the three models exhibited a good performance.

The accuracy of the rock fall hazard zoning was also evaluated by using the seed cell area index (SCAI). SCAI, as the ratio of the area percentage of each rock fall susceptibility class to the frequency percentage of rock fall events in each class, can be calculated by the following equation [64]:

$$SCAI = \frac{\text{Area extent of susceptibility class (\%)}}{\text{Rock fall in each susceptibility class (\%)}} \quad (11)$$

The values required for this evaluation were obtained by using the GIS software to overlay the rock fall event distribution layer onto the rock fall susceptibility zoning map. As shown in Table (5), in all methods, there was a decrease in the SCAI values as we moved from low-susceptibility classes toward the high-susceptibility ones. This indicated a good

correlation between the rock fall susceptibility classes and the high-risk areas observed in the study area. This relationship also showed the acceptable performance of all methods in mapping the susceptibility zones. The trend of change in the SCAI values and the coefficients a and b, as can be seen in Table (5), showed that the FR method had the best performance and that the ANN method outperformed the LR method.

The zoning performance of the methods was also evaluated based on the precision of the predicted results (P). This parameter was calculated by the following equation:

$$P = \frac{K_s}{S} \quad (12)$$

where  $K_s$  is the number of pixel or the area of the rock fall zone at the upper moderate susceptibility zone, and  $S$  is the number of total pixel or the total area of the rock fall zone in the region. As shown in Table (6), the FR, ANN, and LR methods exhibited the precisions (P) of 0.79, 0.92, and 0.74, respectively, indicating the good accuracy of all the three methods in zoning for highly susceptible areas. The P values shown in Table (6) also indicate the higher performance of the ANN method, as compared to the FR and LR methods, in zoning rock fall susceptibility and identifying rock fall susceptible regions in the study area.

Statistical indices performance of developed models for landslide is given in the Table 7. As it obvious, all the models have a proper prediction efficiency. The ANN model yielded the highest efficiency for the categorization of landslide pixels (sensitivity = 91.4%), then the FR model (90.3%), and the LR model (81.7%). The FR model presented the highest specificity, (73.1%), and then the ANN model (67.7%), and the LR model (67.7%). Also, the FR model with the highest accuracy of 81.7% has the best accuracy in predicting landslide and non-landslide pixels, and then ANN model (79.6%), the LR model (74.4%).

## 5. LANDSLIDE MITIGATION AND COUNTERMEASURES

Rockfalls occur in response to one or more external factors in combination with internal conditions causing hillside instability. After determining rockfall susceptibility in an area and identifying effective factors and their impact on a rockfall, some techniques are to be proposed to mitigate the risk. To manage the risk of rockfalls in the study area, the following are suggested:

- Avoidance of new constructions in risk zones, particularly high-risk-prone zones
- Use of suitable approaches of stabilizing the hillsides in order to prevent the rupture of rock blocks and reduce the hazards to the constructions in risk zones by such means as shotcrete, and wire mesh
- Change of land use and creation of green spaces in low-risk-prone zones in order to stop sliding masses and reduce the risk of slips.

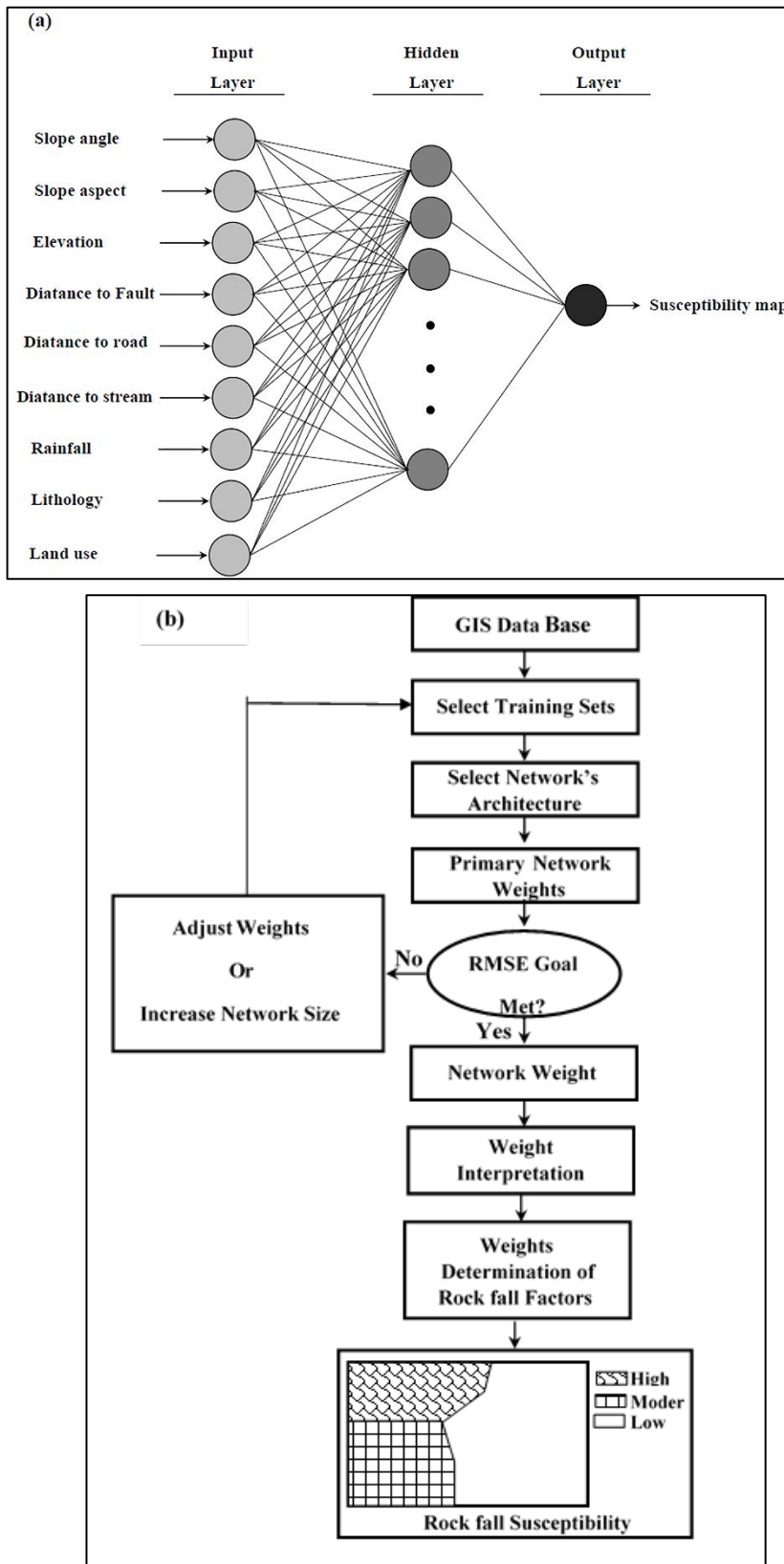


Fig. 6. a) Neural network structure used in the study; b) Rock fall analysis using a neural network

## 6. CONCLUSION

Rock fall is one of the most dangerous natural phenomena in the world, causing many disasters for human beings. A

significant method to diminish future rock fall disasters is to recognize areas prone to rock fall or to prepare rock fall susceptibility maps. Therefore, appropriate regions

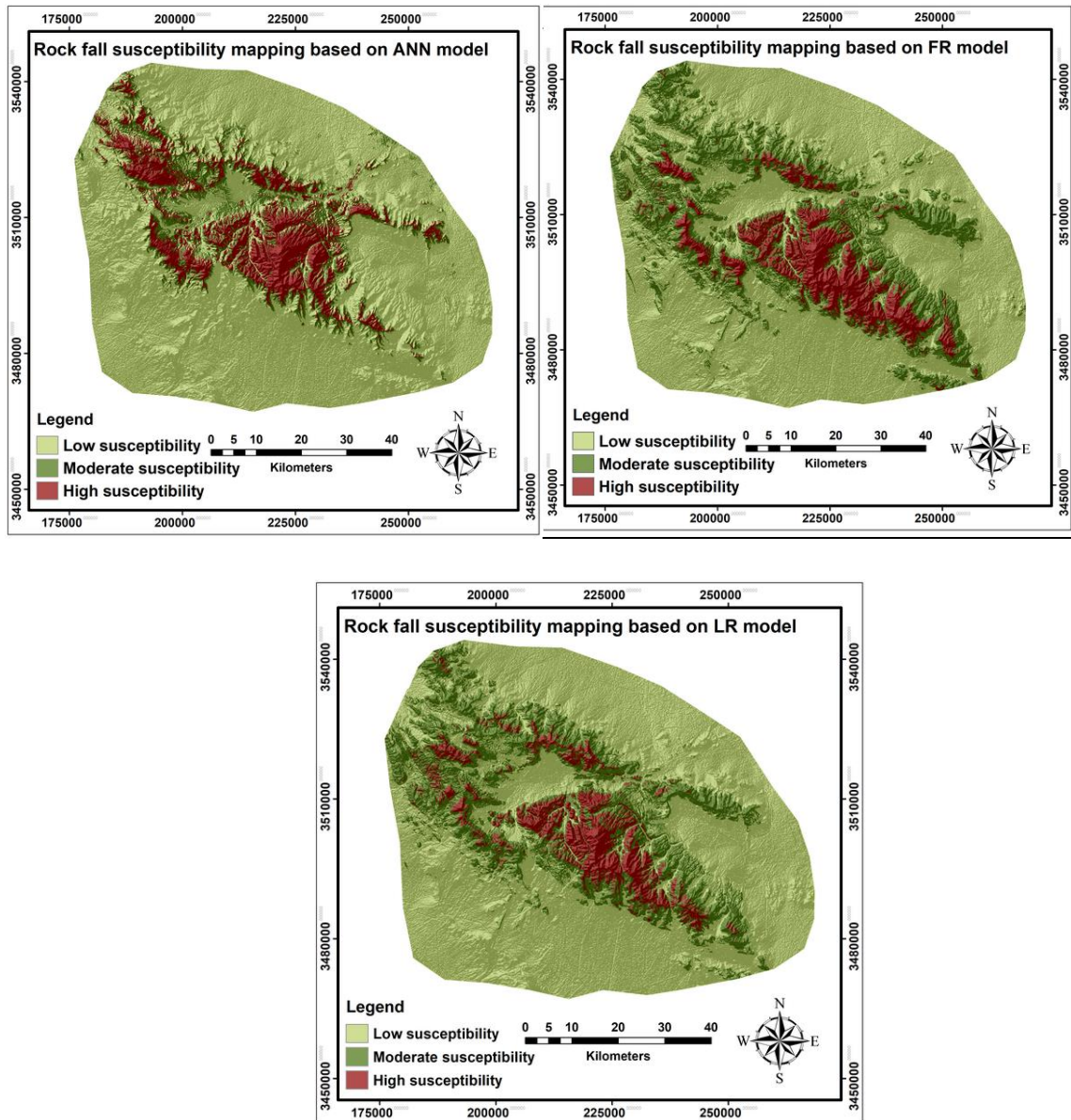


Fig. 7. The rock fall susceptibility map produced by: (a) ANN; (b) FR; (c) LR

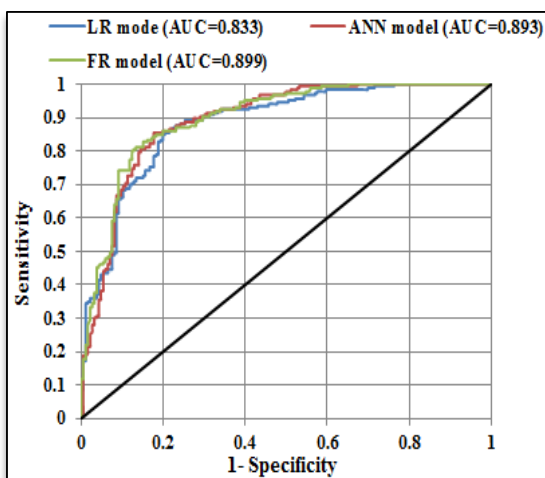


Fig. 8. Assessment of model performance based on the ROC curves

for developmental activities could be identified through determining locations with low rock fall susceptibility. According to this concept, we tried to propose the rock susceptibility planning in this study. FR, ANN, and LR methods were used to obtain the rock fall susceptibility map of the Taft County. Then, the resulting maps were assessed to evaluate the performance of these methods. The research was carried out in three steps including rock fall inventory analysis, rock fall susceptibility mapping, and validation of the resulting maps. The maps were prepared by assuming an association between rock fall susceptibility and nine factors including slope angle, slope aspect, elevation, land use, lithology, rainfall, distance from faults, distance from roads, and distance from streams. The maps prepared by the three models were verified based on the area under the ROC curve (AUC), the SCAI value, and the precision of the predicted results (P). Validation by AUC showed that the areas under

**Table 4. AUC value of the ROC curve in the random sample area**

Method	Area	Std. error <sup>a</sup>	Asymptotic sig. <sup>b</sup>	Asymptotic 95 % confidence interval	
				Upper bound	Lower bound
FR	0.899	0.016	0.0	0.897	0.930
ANN	0.893	0.017	0.0	0.860	0.926
LR	0.883	0.017	0.0	0.849	0.917

<sup>a</sup> Under a nonparametric assumption, <sup>b</sup> Null hypothesis: true area = 0.5

**Table 5. Densities of rock fall in the rock fall-susceptible classes for ANN, FR and LR**

Susceptibility class	ANN			FR			LR		
	a	b	SCAI	a	b	SCAI	a	b	SCAI
Low	80.1	21.01	3.81	98.70	8.20	8.40	88.80	25.60	3.50
Moderate	6.10	8.26	0.71	16.70	15.40	1.10	7.80	34.20	0.20
High	13.80	70.24	0.20	14.50	76.40	0.20	3.40	40.20	0.10

a: % area of predicted class, b: % area of observed rock fall per class (or seed %)

**Table 6. Precision of the predicted results**

Rockfall susceptibility zoning method	Ks <sup>a</sup>	S <sup>b</sup>	P
FR	133543	169053	0.79
ANN	156553	169053	0.92
LR	125754	169053	0.74

a: The number of pixels in the rock fall zone at the upper moderate susceptibility zone

b: The number of total pixels in the rock fall zone

**Table 7. Model validation**

No.	Parameters	ANN	LR	FR
1	True positive	170	152	168
2	True negative	126	126	136
3	False positive	63	60	50
4	False negative	26	34	18
5	Sensitivity (%)	91.40	81.70	90.30
6	Specificity (%)	67.70	67.70	73.10
7	Accuracy (%)	79.60	74.40	81.70

the ROC curves for FR, ANN and LR methods were 0.899, 0.893, and 0.833, respectively, thereby indicating the good performance of all models developed by the employed methods.

Validation by SCAI showed that in all three models, high-susceptibility classes had low SCAI values, but the low-susceptibility ones had higher SCAI values. This relationship indicated the good consistency between rock fall susceptibility maps and rock fall inventory maps. By using statistical techniques, the precision values (P) of the FR, ANN, and LR methods were found to be 0.79, 0.92, and 0.74, respectively. Examining the parameter P, which represented model precision in moderate to high-susceptibility classes, showed that all the three methods had good accuracy in mapping and zoning rock fall susceptible areas. Although the validation results demonstrated the good performance and the high accuracy of all three methods, overall, the FR method proved to outperform. Another objective of the current study was determination of the most important causative factor in

the Taft County. Based on the results of the LR, the rock fall occurrence in the study area had a positive relation with the parameters of slope, slope aspect, elevation, distance to road, distance to fault, and distance to stream, and a negative one with rainfall, lithology and land use. Also, given the amount of coefficients, it could be said that the layer elevation, slope and lithology were the most important factors in the occurrence of rock fall. In the present research, investigations conducted on the zoning of the rock fall risk indicated that in all three models, the probability of rock fall occurrence in the central part of the region was more than that of other areas.

**ACKNOWLEDGEMENT**

Authors are thankful to the Natural Resources and Watershed Management of Yazd province for providing dataset to this research.

**REFERENCES**

- [1] M.J. Selby, Hillslope materials and processes, Oxford University Press, England, 1982.
- [2] G. Abele, Large rockslides: their causes and movement on internal sliding planes, Mountain Research and Development, (1994) 315-320.
- [3] D.J. Varnes, Landslide hazard zonation: a review of principles and practice, Unesco, Paris, 1984.
- [4] B. Pradhan, An assessment of the use of an advanced neural network model with five different training strategies for the preparation of landslide susceptibility maps, Journal of data science, 9(1) (2011) 65-81.
- [5] C. Keylock, U. Domaas, Evaluation of Topographic Models of Rockfall Travel Distance for Use in Hazard Applications, Arctic Antarctic and Alpine Research, 31(3) (1999) 312-320.
- [6] Y. Kobayashi, E.L. Harp, T. Kagawa, Simulation of rockfalls triggered by

- earthquakes, *Rock Mechanics and Rock Engineering*, 23(1) (1990) 1-20.
- [7] K.T. Chau, R.C.H. Wong, J. Liu, C.F. Lee, Rockfall hazard analysis for Hong Kong based on rockfall inventory, *Rock Mech Rock Eng*, 36 (2003) 383-408.
- [8] K. Sassa, H. Fukuoka, G. Wang, N. Ishikawa, Undrained dynamic-loading ring-shear apparatus and application for landslide dynamics, *Landslides*, 1(1) (2004) 7-19.
- [9] M. Fall, R. Azzam, C. Noubactep, A multi-method approach to study the stability of natural slopes and landslide susceptibility mapping, *Engineering geology*, 82(4) (2006) 241-263.
- [10] S. Park, C. Choi, B. Kim, J. Kim, Landslide susceptibility mapping using frequency ratio, analytic hierarchy process, logistic regression, and artificial neural network methods at the Inje area, Korea, *Environmental earth sciences*, 68(5) (2013) 1443-1464.
- [11] F. Dai, C. Lee, Terrain-based mapping of landslide susceptibility using a geographical information system: a case study, *Canadian Geotechnical Journal*, 38(5) (2001) 911-923.
- [12] T.Y. Duman, T. Can, Ö. Emre, M. Keçer, A. Doğan, Ş. Ateş, S. Durmaz, Landslide inventory of northwestern Anatolia, Turkey, *Engineering Geology*, 77(1-2) (2005) 99-114.
- [13] F. Baillifard, M. Jaboyedoff, M. Sartori, Rockfall hazard mapping along a mountainous road in Switzerland using a GIS-based parameter rating approach, *Natural Hazards and Earth System Science*, 3(5) (2003) 435-442.
- [14] F. Guzzetti, P. Reichenbach, S. Ghigi, Rockfall hazard and risk assessment along a transportation corridor in the Nera Valley, Central Italy, *Environmental Management*, 34(2) (2004) 191-208.
- [15] I. Yilmaz, M. Yildirim, Structural and geomorphological aspects of the Kat landslides (Tokat—Turkey) and susceptibility mapping by means of GIS, *Environmental Geology*, 50(4) (2006) 461-472.
- [16] H. Shahabi, M. Hashim, Landslide susceptibility mapping using GIS-based statistical models and Remote sensing data in tropical environment, *Scientific reports*, 5(1) (2015) 1-15.
- [17] A. Shirzadi, K. Chapi, H. Shahabi, K. Solaimani, A. Kavian, B.B. Ahmad, Rock fall susceptibility assessment along a mountainous road: an evaluation of bivariate statistic, analytical hierarchy process and frequency ratio, *Environmental Earth Sciences*, 76(4) (2017) 152-169.
- [18] L. Ayalew, H. Yamagishi, N. Ugawa, Landslide susceptibility mapping using GIS-based weighted linear combination, the case in Tsugawa area of Agano River, Niigata Prefecture, Japan, *Landslides*, 1(1) (2004) 73-81.
- [19] F. Guzzetti, A. Carrara, M. Cardinali, P. Reichenbach, Landslide hazard evaluation: a review of current techniques and their application in a multi-scale study, Central Italy, *Geomorphology*, 31(1) (1999) 181-216.
- [20] H. Kaur, S. Gupta, S. Parkash, Comparative evaluation of various approaches for landslide hazard zoning: a critical review in Indian perspectives, *Spatial Information Research*, 25(3) (2017) 389-398.
- [21] R. Pellicani, I. Argentiero, G. Spilotro, GIS-based predictive models for regional-scale landslide susceptibility assessment and risk mapping along road corridors, *Geomatics, Natural Hazards and Risk*, 8(2) (2017) 1012-1033.
- [22] H. Bourenane, Y. Bouhadad, M.S. Guettouche, M. Braham, GIS-based landslide susceptibility zonation using bivariate statistical and expert approaches in the city of Constantine (Northeast Algeria), *Bulletin of Engineering Geology and the Environment*, 74(2) (2015) 337-355.
- [23] C. Baeza, J. Corominas, Assessment of shallow landslide susceptibility by means of multivariate statistical techniques, *Earth Surface Processes and Landforms: The Journal of the British Geomorphological Research Group*, 26(12) (2001) 1251-1263.
- [24] A.M. Youssef, B. Pradhan, M.N. Jebur, H.M. El-Harbi, Landslide susceptibility mapping using ensemble bivariate and multivariate statistical models in Fayfa area, Saudi Arabia, *Environmental Earth Sciences*, 73(7) (2015) 3745-3761.
- [25] S. Sarkar, A.K. Roy, T.R. Martha, Landslide susceptibility assessment using information value method in parts of the Darjeeling Himalayas, *Journal of the Geological Society of India*, 82(4) (2013) 351-362.
- [26] H. Hong, W. Chen, C. Xu, A.M. Youssef, B. Pradhan, D. Tien Bui, Rainfall-induced landslide susceptibility assessment at the Chongren area (China) using frequency ratio, certainty factor, and index of entropy, *Geocarto international*, 32(2) (2017) 139-154.
- [27] D. Kanungo, S. Sarkar, S. Sharma, Combining neural network with fuzzy, certainty factor and likelihood ratio concepts for spatial prediction of landslides, *Natural hazards*, 59(3) (2011) 1491-1512.
- [28] K.C. Devkota, A.D. Regmi, H.R. Pourghasemi, K. Yoshida, B. Pradhan, I.C. Ryu, M.R. Dhital, O.F. Althuwaynee, Landslide susceptibility mapping using certainty factor, index of entropy and logistic regression models in GIS and their comparison at Mugling–Narayanghat road section in Nepal Himalaya, *Natural hazards*, 65(1) (2013) 135-165.
- [29] H.Y. Hussin, V. Zumpano, P. Reichenbach, S. Sterlacchini, M. Micu, C. van Westen, D. Bălteanu, Different landslide sampling strategies in a grid-based bi-variate statistical susceptibility model, *Geomorphology*, 253 (2016) 508-523.
- [30] H. Hong, I. Ilia, P. Tsangaratos, W. Chen, C. Xu, A hybrid fuzzy weight of evidence method in landslide susceptibility analysis on the Wuyuan area, China, *Geomorphology*, 290 (2017) 1-16.
- [31] G.G. Iovine, R. Greco, S.L. Gariano, A.D. Pellegrino, O.G. Terranova, Shallow-landslide susceptibility in the Costa Viola mountain ridge (southern Calabria, Italy) with considerations on the role of causal factors, *Natural hazards*, 73(1) (2014) 111-136.
- [32] H.R. Pourghasemi, B. Pradhan, C. Gokceoglu, Application of fuzzy logic and analytical hierarchy process (AHP) to landslide susceptibility mapping at Haraz watershed, Iran, *Natural hazards*, 63(2) (2012) 965-996.
- [33] M.H. Tangestani, A comparative study of Dempster–Shafer and fuzzy models for landslide susceptibility mapping using a GIS: An experience from Zagros Mountains, SW Iran, *Journal of Asian Earth Sciences*, 35(1) (2009) 66-73.
- [34] A. Can, G. Dagdelenler, M. Ercanoglu, H. Sonmez, Landslide susceptibility mapping at Ovacık-Karabük (Turkey) using different artificial neural network models: comparison of training algorithms, *Bulletin of Engineering Geology and the Environment*, 78(1) (2017) 1-14.
- [35] I. Yilmaz, A case study from Koyulhisar (Sivas-Turkey) for landslide susceptibility mapping by artificial neural networks, *Bulletin of Engineering Geology and the Environment*, 68(3) (2009) 297-306.
- [36] W. Chen, H.R. Pourghasemi, S.A. Naghibi, A comparative study of landslide susceptibility maps produced using support vector machine with different kernel functions and entropy data mining models in China, *Bulletin of Engineering Geology and the Environment*, 77(2) (2018) 647-664.
- [37] H. Hong, B. Pradhan, M.I. Sameen, W. Chen, C. Xu, Spatial prediction of rotational landslide using geographically weighted regression, logistic regression, and support vector machine models in Xing Guo area (China), *Geomatics, Natural Hazards and Risk*, 8(2) (2017) 1997-2022.
- [38] D.T. Bui, B. Pradhan, O. Lofman, I. Revhaug, O.B. Dick, Landslide susceptibility mapping at Hoa Binh province (Vietnam) using an adaptive neuro-fuzzy inference system and GIS, *Computers & Geosciences*, 45 (2012) 199-211.
- [39] C. Polykretis, C. Chalkias, M. Ferentinou, Adaptive neuro-fuzzy inference system (ANFIS) modeling for landslide susceptibility assessment in a Mediterranean hilly area, *Bulletin of Engineering Geology and the Environment*, 78(2) (2017) 1-15.
- [40] N. Jia, Y. Mitani, M. Xie, I. Djameluddin, Shallow landslide hazard assessment using a three-dimensional deterministic model in a mountainous area, *Computers and Geotechnics*, 45 (2012) 1-10.
- [41] H. Saroglou, V. Marinos, P. Marinos, G. Tsiambaos, Rockfall hazard and risk assessment: an example from a high promontory at the historical site of Monemvasia, Greece, *Natural Hazards and Earth System Sciences*, 12(6) (2012) 1823-1836.
- [42] D.T. Bui, B. Pradhan, O. Lofman, I. Revhaug, O.B. Dick, Spatial prediction of landslide hazards in Hoa Binh province (Vietnam): a comparative assessment of the efficacy of evidential belief functions and fuzzy logic models, *Catena*, 96 (2012) 28-40.
- [43] D.G. Price, *Engineering geology: principles and practice*, Springer, (2009) 268-290.
- [44] P. Magliulo, A. Di Lisio, F. Russo, A. Zelano, Geomorphology and landslide susceptibility assessment using GIS and bivariate statistics: a case study in southern Italy, *Natural hazards*, 47(3) (2008) 411-435.
- [45] A.R. Arabameri, A.H. Halabian, Landslide Hazard Zonation Using

- Statistical Model of AHP (Case Study: Zarand Saveh Basin), *Physical Geomorphology*, 28 (2015) 65-86.
- [46] R. Giannecchini, Relationship between rainfall and shallow landslides in the southern Apuan Alps (Italy), *Natural Hazards and Earth System Science*, 6(3) (2006) 357-364.
- [47] C. Henriques, J.L. Zêzere, F. Marques, F. Marques, The role of the lithological setting on the landslide pattern and distribution, *Engineering Geology*, 189 (2015) 17-31.
- [48] H.R. Pourghasemi, M. Mohammady, B. Pradhan, Landslide susceptibility mapping using index of entropy and conditional probability models in GIS: Safarood Basin, Iran, *Catena*, 47(3) (2012) 411-435.
- [49] A.M. Youssef, H.R. Pourghasemi, Z.S. Pourtaghi, M.M. Al-Katheeri, Landslide susceptibility mapping using random forest, boosted regression tree, classification and regression tree, and general linear models and comparison of their performance at Wadi Tayyah Basin, Asir Region, Saudi Arabia, *Landslides*, 13(5) (2016) 839-856.
- [50] A. Moteashari, J. Qomi, A. Eftekhari, B. Puzesh, M. Shahmari, Landslide hazard zoning of the Tehran-Chalus road and the highway under construction, *Applied Geology*, 8 (2012) 147-158.
- [51] T. Kavzoglu, E. Sahin, I. Colkesen, Landslide susceptibility mapping using GIS-based multi-criteria decision analysis, support vector machines, and logistic regression, *Landslides*, 11(3) (2013) 425-439.
- [52] D. Tien Bui, O. Lofman, I. Revhaug, O. Dick, Landslide susceptibility analysis in the Hoa Binh province of Vietnam using statistical index and logistic regression, *Nat Hazards*, 59(3) (2011) 1413-1444.
- [53] H. Gomez, T. Kavzoglu, Assessment of shallow landslide susceptibility using artificial neural networks in Jabonosa River Basin, Venezuela, *Engineering Geology*, 78(1-2) (2005) 11-27.
- [54] M. Zare, H.R. Pourghasemi, M. Vafakhah, B. Pradhan, Landslide susceptibility mapping at Vaz Watershed (Iran) using an artificial neural network model: a comparison between multilayer perceptron (MLP) and radial basic function (RBF) algorithms, *Arabian Journal of Geosciences*, 6(8) (2013) 2873-2888.
- [55] J. Paola, R. Schowengerdt, A review and analysis of backpropagation neural networks for classification of remotely-sensed multi-spectral imagery, *International Journal of remote sensing*, 16(16) (1995) 3033-3058.
- [56] B. Pradhan, S. Lee, Landslide susceptibility assessment and factor effect analysis: backpropagation artificial neural networks and their comparison with frequency ratio and bivariate logistic regression modelling, *Environmental Modelling & Software*, 25(6) (2010) 747-759.
- [57] S. Lee, Application of likelihood ratio and logistic regression models to landslide susceptibility mapping using GIS, *Environmental Management*, 34(2) (2004) 223-232.
- [58] X. Deng, L. Li, Y. Tan, Validation of spatial prediction models for landslide susceptibility mapping by considering structural similarity, *ISPRS International Journal of Geo-Information*, 6(4) (2017) 103-119.
- [59] M.J. García-Rodríguez, J. Malpica, B. Benito, M. Díaz, Susceptibility assessment of earthquake-triggered landslides in El Salvador using logistic regression, *Geomorphology*, 95(3-4) (2008) 172-191.
- [60] S. Lee, T. Sambath, Landslide susceptibility mapping in the Damrei Romel area, Cambodia using frequency ratio and logistic regression models, *Environmental Geology*, 50(6) (2006) 847-855.
- [61] L. Ayalew, H. Yamagishi, The application of GIS-based logistic regression for landslide susceptibility mapping in the Kakuda–Yahiko Mountains, Central Japan, *Geomorphology*, 65(1-2) (2005) 15-31.
- [62] F. Cervi, M. Berti, L. Borgatti, F. Ronchetti, F. Manenti, A. Corsini, Comparing predictive capability of statistical and deterministic methods for landslide susceptibility mapping: a case study in the northern Apennines (Reggio Emilia Province, Italy), *Landslides*, 7(4) (2010) 433-444.
- [63] M.H.A. Hasanat, D. Ramachandram, R. Mandava, Bayesian belief network learning algorithms for modeling contextual relationships in natural imagery: a comparative study, *Artificial Intelligence Review*, 34(4) (2010) 291-308.
- [64] M.L. Süzen, V. Doyuran, A comparison of the GIS based landslide susceptibility assessment methods: multivariate versus bivariate, *Environmental geology*, 45(5) (2004) 665-679.

#### HOW TO CITE THIS ARTICLE

M. Mokhtari, S. Abedian, S.A. Almasi, *Rock fall Susceptibility Mapping Using Artificial Neural Network, Frequency Ratio, and Logistic Regression: A Case Study in Central Iran, Taft County*, *AUT J. Civil Eng.*, 4(1) (2020) 63-80.

DOI: [10.22060/ajce.2019.15368.5538](https://doi.org/10.22060/ajce.2019.15368.5538)



